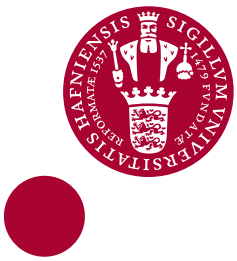

Ecological engineering projects increased vegetation cover, production, and biomass in semiarid and subhumid Northern China

Niu, Quanfu; Xiao, Xiangming; Zhang, Yao; Qin, Yuanwei; Dang, Xinghai; Wang, Jie; Zou, Zhenhua; Doughty, Russell B.; Brandt, Martin; Tong, Xiaowei; Horion, Stephanie; Fensholt, Rasmus; Chen, Chi; Myneni, Ranga B.; Xu, Weiheng; Di, Guangzhi; Zhou, Xiaoming

Published in:
Land Degradation & Development

DOI:
10.1002/ldr.3351

Publication date:
2019

Document version
Peer reviewed version

Ecological engineering projects increased vegetation cover, production, and biomass in semiarid and subhumid Northern China

Quanfu Niu[1,2,3] | Xiangming Xiao[2,4] | Yao Zhang[2,5] | Yuanwei Qin[2] | Xinghai Dang[1] | Jie Wang[2] | Zhenhua Zou[2] | Russell B. Doughty[2] | Martin Brandt[6] | Xiaowei Tong[7] | Stephanie Horion[6] | Rasmus Fensholt[6] | Chi Chen[8] | Ranga B. Myneni[8] | Weiheng Xu[9] | Guangzhi Di[9] | Xiaoming Zhou[1]

[1] School of Civil Engineering, Lanzhou University of Technology, Lanzhou 730050, PR China [2] Department of Microbiology and Plant Biology and Center for Spatial Analysis, University of Oklahoma, Norman, OK 73019, USA [3] Emergency Mapping Engineering Reseach Center, Gansu Province, Lanzhou 730050, PR China [4] Ministry of Education Key Laboratory for Biodiversity Science and Ecological Engineering, Institute of Biodiversity Science, Fudan University, Shanghai 200433, PR China [5] Department of Earth and Environmental Engineering, Columbia University, New York, NY 10027, USA [6] Department of Geosciences and Natural Resource Management, University of Copenhagen, Copenhagen 1350, Denmark [7] Key Laboratory for Agro-ecological Processes in Subtropical Region, Institute of Subtropical Agriculture, Chinese Academy of Sciences, Changsha 410125, PR China [8] Department of Geography, Boston University, Commonwealth avenue, Boston, MA 02215, USA [9] College of Big Data and Intelligent Engineering, Southwest Forestry University, Kunming 650224, PR China

Correspondence Xiangming Xiao, Department of Microbiology and Plant Biology and Center for Spatial Analysis, University of Oklahoma, Norman, OK 73019. Email: xiangming.xiao@ou.edu

Abstract

Multiple ecological engineering projects have been implemented in semiarid and subhumid Northern China since 1978 with the purpose to combat desertification, control dust storms, and improve vegetation cover. Although a plethora of local studies exist, the effectiveness of these projects has not been studied in a systematic and comprehensive way. Here, we used multiple satellite-based time-series data as well as breakpoint analysis to assess shifts in leaf area index (a proxy for green vegetation cover), gross primary production, and aboveground biomass in Northern China. We documented increased vegetation growth in northwest and southeastern parts of the region, despite drought anomalies as documented by the standardized precipitation-evapotranspiration index during 1982–2016. Significant breakpoints in leaf area index were observed for over 72.5% of the southeastern and northwestern regions, and 70.6% of these breakpoints were detected after 1999, which correspond well to the areas with the highest ecological engineering efforts. Areas with negative trends were mainly located in the Inner Mongolian Plateau, Hulun Biur, Horqin Sand Land, and urban areas. The Loess Plateau had the largest increase in vegetation

growth, followed by the north parts of Northern China where biomass increased more in the provinces of Shanxi, Liaoning, Shannxi, Hebei, and Beijing than Xinjiang, Inner Mongolia, Tianjin, and Qinghai. Our results show that multiple ecological engineering projects in the region have increased vegetation cover, production, and aboveground biomass that have led to improved environmental conditions in the study area.

Keywords: breakpoint, effectiveness, remote sensing, trend, vegetation regrowth

1 INTRODUCTION

Forest resources in China are characterized by an inadequate supply, low-quality, and uneven geographic distribution, especially in the semiarid and subhumid areas of Northern China (China Forestry Administration, 1987). For several centuries, more than 60% of the region has been managed by traditional pastoral and agricultural systems (Wang, Zhang, Hasi, & Dong, 2010). Rapid population growth, coupled with fast economic development have, resulted in an enormous demand for forest resources, which has led to hillside deforestation in the upper and middle reaches of the Yangtze and Yellow River basins. Such changes in woody cover increased the intensity of water runoff and soil erosion and a decline in the ecosystem's capacity to regulate water and hold soil in place (Xu, Yin, Li, & Liu, 2006). Various environmental problems, such as land degradation, dust storms, and soil erosion, are the clear signs of an imbalance between human management and natural conditions in Northern China (Zhu, 1998). Several ecological research projects during recent decades have focused on environmental changes in Northern China (Qiu et al., 2017; Wu et al., 2014; Yu, Li, & Li, 2006; X. Zhang et al., 2016; Y. Zhang et al., 2016), and to combat environmental problems, the Chinese Government has launched several large-scale ecological engineering projects (EEPs). The largest EEP afforestation effort is the Three-North Shelter Forest Program (TNSFP), aimed at increasing forest cover in the region from 5% to 15% between 1978 and 2050 (Wang et al., 2010). The EEP with the largest economic investment from the Chinese Government is the Grain for Green Program (GfG), which is a major ecological project with the widest coverage (e.g., TNSFP is a subset of GfG) and has the highest rate of public participation in history, involving 124 million people and 32 million households in a total of 1,897 counties and 25 provinces (Delang & Wang, 2013; Delang & Yuan, 2015; Zhou, Gan, Shangguan, & Dong, 2009). Other EEPs in the region have been launched by the Chinese Government to address different environment problems in the region, such as weakening sandstorms around Beijing and Tianjin and flooding and soil erosion in the upper reaches of the Yangtze and Yellow Rivers. These other EEPs include the Beijing-Tianjin Sand Source Control Program (BSSCP) and the Natural Forest Conservation Program (NFCP) and are expected to remarkably speed up the restoration of the forest ecosystems. Important afforestation achievements have been reported by

governmental bulletins, forestry statistical yearbooks, and previous studies (Yu et al., 2006; Y. Zhang et al., 2016).

Although these large-scale EEPs have been carried out unceasingly in the region, several studies have questioned the effectiveness of vegetation restoration. For instance, some studies found that desertification and dust storms weakened substantially as vegetation cover increased (Fan et al., 2014; Piao et al., 2015; Tan & Li, 2015) and that the regional climate also had a positive feedback (Jiang, Liang, & Yuan, 2015; Qiu et al., 2017; Y. Zhang et al., 2016). However, other researchers questioned the effectiveness of planting trees in dry regions because of low precipitation (Cao, 2008; Cao & Wang, 2010; Ma, Lv, & Li, 2013; Sun et al., 2006). Most studies on these large-scale EEPs only considered a single parameter of vegetation (e.g., normalized difference vegetation index [NDVI]) in a limited area (Chen et al., 2014; Wu et al., 2014; X. Zhang et al., 2016; Y. Zhang et al., 2016). Due to the large span from east to west, the complexity of the terrain, the differences in climate in the region, and the long implementation time of the EEPs, their ecological effects usually show their impact after a long period of time. Hence, systemic assessments about the programme's effect in the long-term and whole region become imperative.

The effectiveness of vegetation restoration can be accurately measured with long-term records of vegetation indices from satellite-based image. NDVI can represent variability in the photosynthetic capacity of the vegetation (Neigh, Tucker, & Townshend, 2008) and has been widely used to monitor vegetation dynamics (Chen, Marter-Kenyon, Lopez-Carr, & Liang, 2015; Eckert, Hüsler, Liniger, & Hodel, 2015; Fensholt et al., 2012; Piao, 2003; Piao et al., 2014). In recent studies, global leaf area index (LAI; a proxy for green vegetation cover), aboveground biomass (AGB) carbon, vegetation optical depth (VOD), and gross primary production (GPP), and net primary production of vegetation were also used to monitor vegetation dynamics (Liu et al., 2015; Piao et al., 2015; Schaphoff et al., 2017; Tong et al., 2018; Xiao, 2004; Zhang et al., 2017; Zhu et al., 2016). To obtain the long-term trends, time-series analysis of vegetation indices is commonly used to model changes and trends in vegetation response to disturbances (Brandt et al., 2015; de Jong, de Bruin, de Wit, Schaepman, & Dent, 2011; Piao et al., 2015; Weiss, Gutzler, Coonrod, & Dahm, 2004). Many temporal analysis algorithms have been developed to identify the phenological indicators (Galford et al., 2008; Jönsson & Eklundh, 2002), the trend analysis and other statistics from a decomposed time-series (Hill & Donald, 2003; Y. Zhang et al., 2016). The Breaks for Additive Season and Trend (BFAST) algorithm has been used to identify long-term trends and abrupt changes (breaks) in time-series (de Jong, Verbesselt, Zeileis, & Schaepman, 2013; Tong et al., 2018; Verbesselt, Hyndman, Zeileis, & Culvenor, 2010). Therefore, time-series analysis with multivariable (parameters) and effective algorithms are critically needed to comprehensively assess the effectiveness of vegetation restoration that will

provide essential data, information, and knowledge for us to better implement and manage large-scale EEPs.

The temporal dynamics of terrestrial ecosystems in our study region commonly consist of continuous (gradual), discontinuous (abrupt) changes, and more rarely, no change. And the trigger factors also include precipitation, diseases, and human management (deforestation and afforestation). Identifying where and when a trend shift in vegetation dynamics occurred and how and how much the vegetation changed combining with EEPs is important for better implementation of large-scale EEPs. Hence, in this study, we conducted a time-series analysis using multidecade satellite images, climate data, and statistical data to (a) quantify the changes in LAI, AGB, and GPP of vegetation in the region and (b) compare the changes in vegetation with the implementation times of large-scale EEPs and assess the effectiveness of EEPs on vegetation structure and function in Northern China.

2 MATERIALS AND METHODS

2.1 Study area

Northern China is an inland region (34°20′ N–50°11′ N and 73°27′ E–128°13′ E) in Eurasia. This region (4.1 million km^2) consists of 590 counties within 13 provinces and accounts for ~42.4% of China's territory (Figure 1). It runs more than 4,480 km from east to west and 560–1,460 km from south to north, and environmental conditions and vegetation are considerably diverse (Zhu, Liu, & Di, 1989). For example, annual mean temperature ranges from −2° (northeast) to 14° (southwest), annual precipitation decreases from east (800 mm) to west (25 mm; Wang et al., 2010), and moisture conditions vary from semihumid to semiarid (middle) and arid (west; Xu & Zou, 1998). The natural vegetation types that are largely determined by precipitation, transitions from east to west from meadow steppes, typical steppes, desert steppes, the Gobi Desert to the typical desert (Zheng & Zhu, 2013). The range of the TNSFP was divided into four subregions according to geography and land cover: western Northeast China (WNS), north Northern China (NNS), the Loess Plateau (LPS), and the Mongolia-Xinjiang subregion (MXS; China Forestry Administration, 1987).

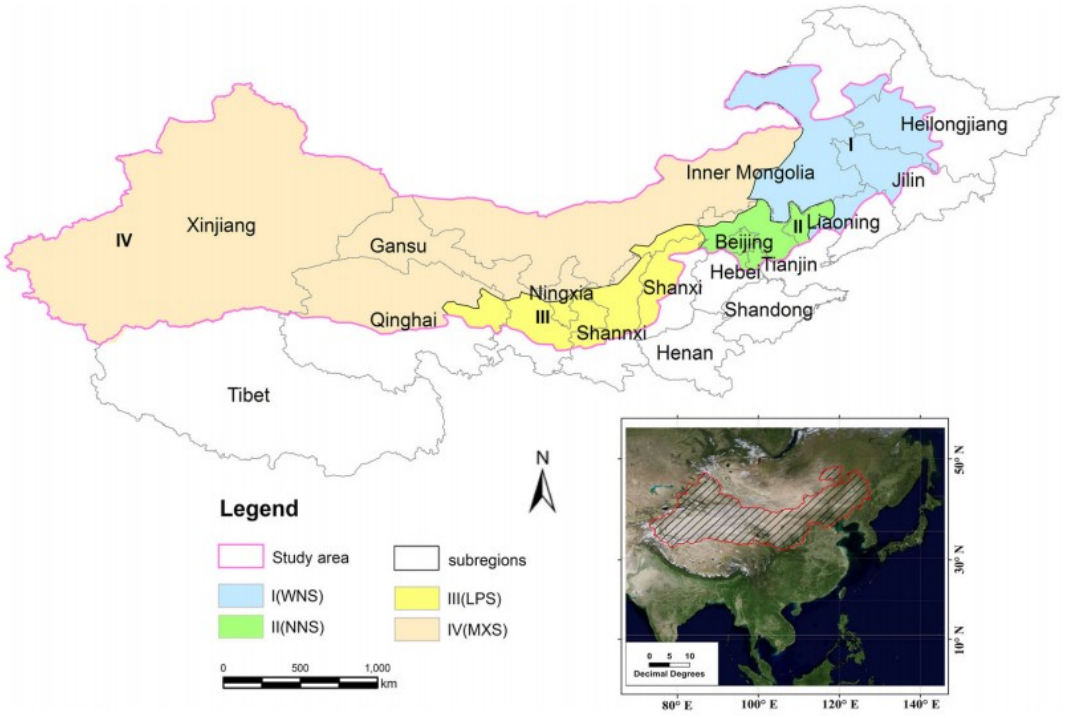

Figure 1. Study area in Northern China (mainly including the Three-North Shelter Forest Program), defined also by the shadow line in the inner figure (right lower corner of Figure 1). I, western Northeast China (WNS.); II, Northern North China (NNS); III, the Loess Plateau (LPS); and IV, Mongolia-Xinjiang (MXS)

2.2 Inventory data on large-scale EEPs

We used the statistical data (mainly afforestation area at provincial level) from multiple national EEPs including the TNSFP, GfG, NFCP, and BSSCP (Figure S1). The TNSFP is the largest afforestation project and the most distinctive EEP in China (Li et al., 2012). The primary aim of the TNSFP is to combat desertification, weaken dust storms, and improve forest cover through extensive afforestation. TNSFP is planned to be fully implemented as a sequence of eight engineering schedules during three periods (1978–2000, 2001–2020, and 2021–2050; Li et al., 2012). The tasks of the first period (1978–2000) and the fourth schedule (2001–2010) in the second period have been completed, and a forest cover increase from 5% in 1978 to 10% was reported in 2010 (Wang et al., 2010). The GfG was put in place in 1999 primarily to reconvert steep slopes (>25°) that had previously been cleared for farming in the countryside to ecological and economical forests or grasslands (Chen et al., 2015; Delang & Yuan, 2015; Zhou et al., 2009). Upon completion of GfG, the forest and grass cover of the target areas should increase by 5%, and most soil- and water-eroded and sand-fixation areas are expected to be under control. The BSSCP was launched in 1993, and it was expected to remarkably improve the ecosystems and living conditions around Beijing and Tianjin. The NFCP was started in 1999 following the devastating floods in 1998 in China, and its aim is mainly to reduce the logging in natural forests, plant trees on barren hills, and uncultivated land in

the region of upper Yangtze River, middle and upper of Yellow River. The province level inventory data, including implementation areas of all EEPs, from 1982 to 2016 were collected from the China forestry yearbooks (Table S1).

2.3 Satellite-based data products

Multiple long-term data sets were used to monitor the impact of EEPs on changes in LAI, GPP, and AGB.

2.3.1 Third-generation Global Inventory Modeling and Mapping Studies LAI

The third-generation Global Inventory Modeling and Mapping Studies (GIMMS-3g) LAI data set was generated from the (GIMMS-3g) NDVI based on an algorithm using artificial neutral network. The artificial neutral network was trained by LAI from Terra Moderate Resolution Imaging Spectroradiometer (MODIS) and GIMMS-3g NDVI (Zhu et al., 2013). The GIMMS-3g LAI data set has a 1/12° spatial resolution and a 15-day temporal frequency from 1982 to 2016. We averaged the growing season LAI data (from April to September) over each year to characterize the annual vegetation greenness in the study region (Fernandes, Butson, Leblanc, & Latifovic, 2003; Zhu et al., 2013).

2.3.2 MODIS gross primary production

The GPP data set from the Vegetation Photosynthesis Model (hereafter GPP_{VPM}) is produced by using MODIS surface reflectance (MOD09A1) and climate data from NCEP Reanalysis II (Xiao, 2004; Xiao, Zhang, Hollinger, Aber, & Moore, 2005). The GPP_{VPM} data set has a moderate spatial (500 m) and temporal (8-day) resolution and ranges from 2000 to 2016 (Zhang et al., 2017). Annual total and mean GPP data were calculated and used for this study. The GPP_{VPM} data set is available to the public at https://doi.pangaea.de/10.1594/PANGAEA.879560.

2.3.3 VOD aboveground biomass

VOD, derived from passive microwaves, is sensitive to the water content of all photosynthetic and nonphotosynthetic parts of vegetation (Tian et al., 2016), less prone to saturation, less sensitive to interannual variations in climate, and almost insensitive to clouds. Thus, it has been widely used as an indicator to estimate AGB (Brandt et al., 2018; Liu et al., 2015). The monthly long-term VOD (1992–2012) data set we used was provided in a spatial resolution of 0.25° × 0.25° and values ranged from 0 to ~1.3 (Liu, de Jeu, McCabe, Evans, & van Dijk, 2011). We used the VOD as a proxy for aboveground biomass and additionally carbon stocks (C stocks) of the entire study area. Here, we established a relationship between a global biomass carbon benchmark map and annual mean VOD to convert VOD to the unit MgC^{-1} ha^{-1} following Liu et al. (2015) and Tong et al. (2018). By summing the values of pixels of the study area, we estimated annual C stocks.

2.4 Climate data

We used the monthly global gridded standardized precipitation-evapotranspiration index (SPEI) data set that provides long-term, robust information on drought conditions at a 0.5° × 0.5° spatial resolution (Vicente-Serrano et al., 2017). Our study focuses on vegetation change that usually involves lagged response times to fluctuations in rainfall, so we used 6-month SPEI data. The annual average SPEI was calculated to analyze the effect of climate on vegetation dynamics. We also used monthly average precipitation and temperature data from 198 meteorological stations in study region from 1981 to 2010 to analyze the relationship between vegetation parameters and precipitation and temperature.

2.5 Statistical analysis

2.5.1 Breakpoint dynamic analysis

The BFAST algorithm decomposes a time-series into seasonal, trend, and irregular components and iteratively fits piecewise a linear trend and seasonal models to a time-series (Cleveland, Cleveland, McRae, & Terpenning, 1990; Verbesselt, Hyndman, Newnham, & Culvenor, 2010). It was used to detect long-term trends and abrupt changes (breaks; de Jong et al., 2013; Verbesselt, Hyndman, Zeileis, et al., 2010). We used GIMMS-3g LAI data as a basis for detecting and analyzing breakpoints because of its long temporal availability and reasonable spatial resolution (de Jong et al., 2013; Tong et al., 2018). Breakpoints in LAI time-series can be caused by various factors (such as climate and management), including the potential impact from initiation of EEPs. We thus analyzed the vegetation changes by comparing the patterns of detected breakpoints with climate data and the timing of these EEPs implementations.

2.5.2 Trend analysis

An ordinary least square regression was used to calculate the slope, intercept, and *p* value in satellite-observed time-series to assess vegetation changes in Northern China because this approach is simple and computationally efficient. The vegetation changes were mainly characterized using the slope value, which expresses the change in the corresponding unit per year. The *p* value was used to single out significant trends. All these methods and statistical analysis were conducted in the R program (Chambers, 2009).

3 RESULTS

3.1 Breakpoint detection from LAI data

Most of the breakpoints detected by BFAST in the GIMMS-3g LAI time-series were in the eastern region of the study area (Figure 2), and seven major breakpoint classes were identified (Figure S2). A majority of the breakpoints (pixels) were observed to be positive with the class of monotonic increase accounting for 72.5% of the study area, and pixels with a monotonic increase showing a positive break and monotonic increases showing a negative break

(interruption: increase with negative break) cover 3.5% and 5.4% of the study area, respectively. Contrarily, monotonic decrease covered 16.3% and monotonic decrease with positive break (interruption: decrease with positive break) covered 0.3%. No pixels had a monotonic decrease with a negative break. Pixels that changed from an increase to decrease and from decrease to increase covered 0.6% and 1.4%, respectively (Figure 2a). From the spatial distribution of the breakpoint year (Figure 2b), the timing of the breakpoints can be observed to shift toward a later breakpoint year from south to north, which reflects the vegetation dynamics in the region expanding successively to the north during our study period. About 11.1% of the breakpoints were detected and located in south and southeast of the study area because of limited data availability prior to 1993. Then, an obvious increase of number of breakpoints was observed in 1993–2006, stabilizing during the years 2006–2008. In total, 70.6% of the breakpoint pixels were detected in study period after 1999. Many breakpoints were identified in 1999–2002, accounting for 22.4% of the total breakpoints. At that time, all large-scale EEPs were being actively implemented (Tables 1), especially in 2000. The total area of all EEPs was 3.17×10^6 ha, with GfG accounting for 3.04×10^6 ha, which contributed to the number of breakpoints.

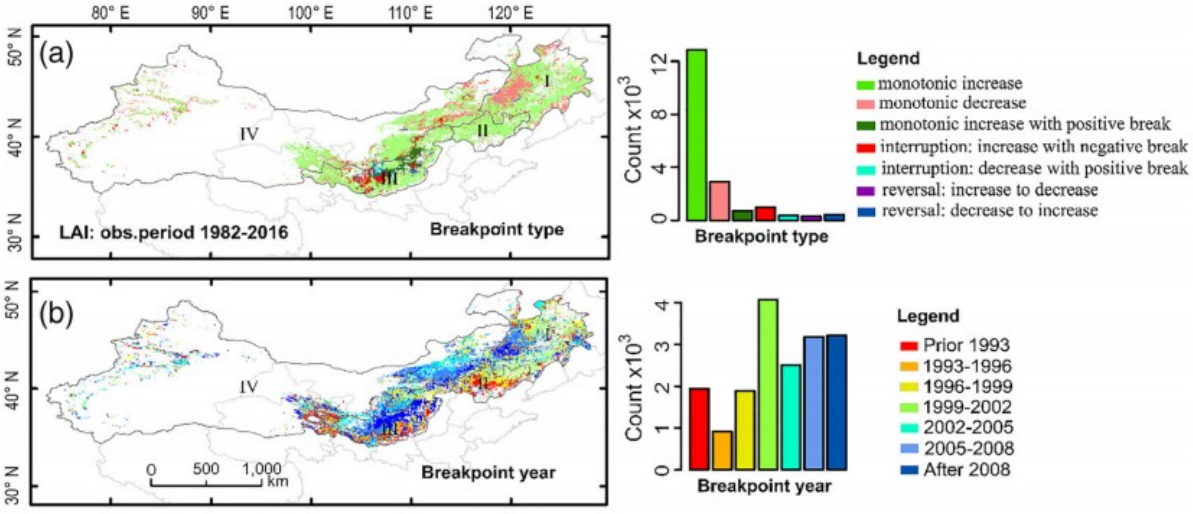

Figure 2. Spatial distribution of per-pixel leaf area index (LAI) breakpoints detected by Breaks for Additive Season and Trend (BFAST). (a) Spatial distribution of seven breakpoint classes. (b) Spatial distribution of the year of breakpoint detection

TABLE 1 Average trends of LAI, GPP_{VPM}, and C stocks at the subregional level

	LAI trends (m^2 m^{-2} yr^{-1})			GPP_{VPM} trends (gC yr^{-2})	C stocks trends (TgC yr^{-1})		
Subregions	Pre-1999	Post-1999	ΔLAI trend	Post-1999	Pre-1999	Post-1999	ΔC trend
WNS (I)	0.038	0.043	0.005	4.9	−0.0004	0.188	0.1884
NNS (II)	0.05	0.06	0.01	6.1	−0.0002	0.733	0.7332
LPS (III)	0.036	0.07	0.034	7.2	−0.0003	0.609	0.6093
MXS (IV)	0.04	0.031	−0.09	2.3	−0.0001	0.025	0.0251

Abbreviations: GPP_{VPM}, gross primary production data set from the Vegetation Photosynthesis Model; LAI, leaf area index; LPS. Loess Plateau; MXS, Mongolia-Xinjiang subregion; NNS, Northern North China; WNS, western Northeast China.

The number of breakpoints detected from LAI time-series showed a decrease at first and then an increasing trend around 1999 (Figure 3a,c), which is consistent with the trend from SPIE (Figure 3h). Meanwhile, the breakpoints in the 2000s are obviously higher than those before and corresponded to the period when the EEPs were implemented (Figure 3b,d). The time-series LAI (1982–2016) reveals that TNSFP had minor impacts on LAI breakpoints during the 1980s and 1990s, and only when the GfG and other EEPs (starting in 1999) began, a more significant number of breakpoints in LAI occurred. The breakpoints also shifted with plantation area caused by the EEPs in the region, and the significant breakpoints after 2000 lagged behind the effort of the EEPs, likely due to the lag effect caused by vegetation growth.

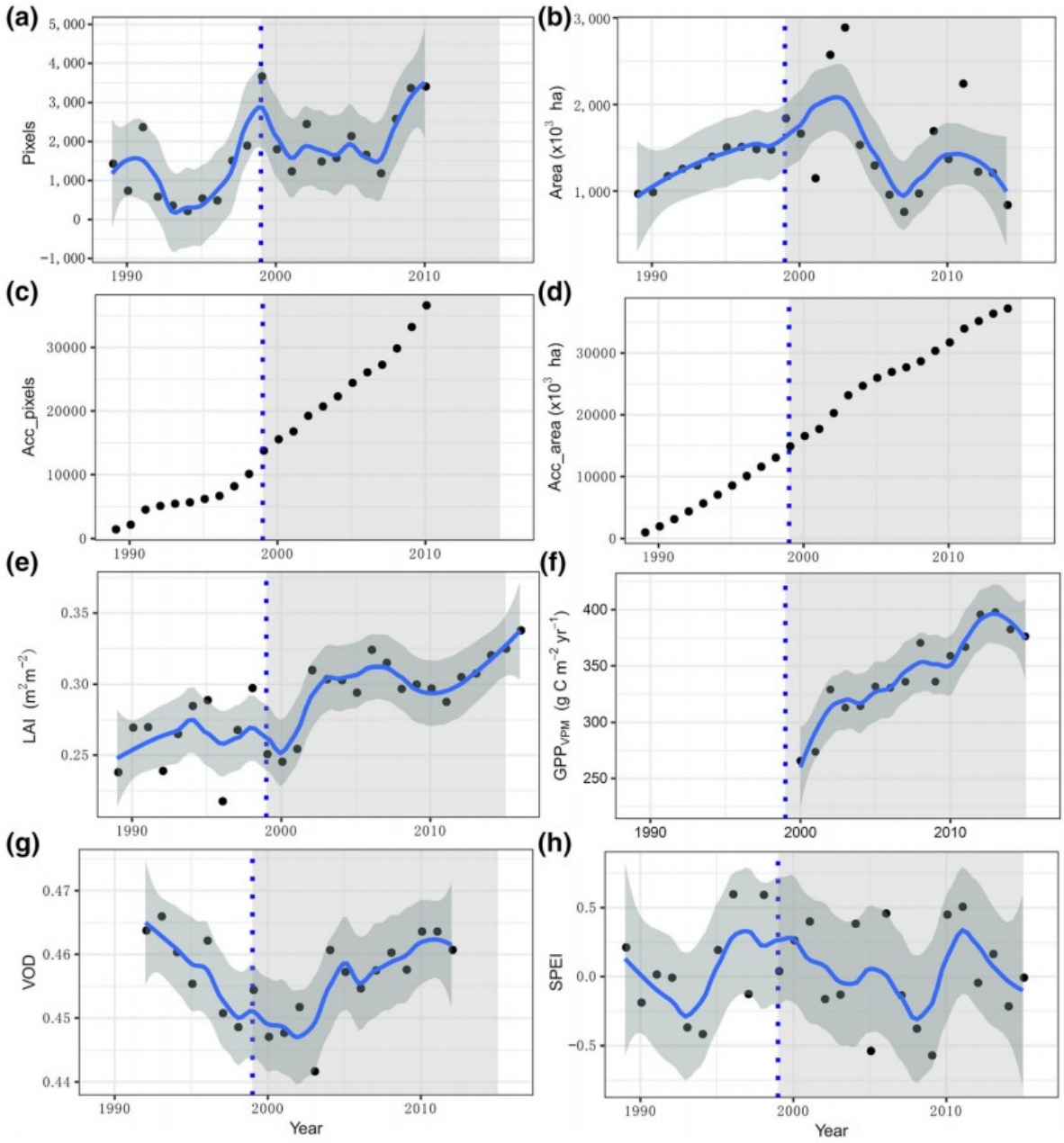

Figure 3. Temporal profiles of multiple time-series data in the study area. (a) Pixel breakpoints from leaf area index (LAI; 1989–2010). (b) Plantation areas (1989–2014). (c) Accumulated breakpoint pixels. (d) Accumulated plantation areas. (e) Annual average third-generation Global Inventory Modeling and Mapping Studies LAI (1982–2016). (f) Annual sum GPP data set from the Vegetation Photosynthesis Model (GPP_{VPM}; 2000–2016). (g) Annual average vegetation optical depth (VOD; 1992–2012). (h) Annual average standardized precipitation-evapotranspiration index (SPEI; 1982–2015)

3.2 Annual dynamics of LAI, GPP_{VPM}, and VOD time-series

Annual dynamics from these time-series data for the region were illustrated in Figure 3. Before 1999, annual average LAI had a weak positive trend (β = +.001 m^2 m^{-2} yr^{-1}, $p < .5$; Figure 3e). After 1999, annual average GPP_{VPM} (not available before 2000), VOD, and LAI all had positive temporal trends (Figure

3e–g). LAI increased three times faster (β = +.003 m^2 m^{-2} yr^{-1}, p < .05) after 1999, and GPP_{VPM} increased strongly from 2000 to 2016 (β = +7.5 gC yr^{-1}, p < .001). Annual dynamics of VOD-based AGB during 1992–2012 changed from a decreasing trend (β = −.002, p < .003) in 1992–1999 to an increasing trend (β = .002, p < 0.0) during 2000–2012 (Figure 3g). Two drought periods were identified from the SPEI data (1993–1994 and 2007–2009; Figure 3h). The rather neutral LAI and the decrease in VOD before 1999 could be a sign of insufficient project efforts (the period the TNSFP was already implemented) that were additionally offset by the effects of severe droughts (Chen & Sun, 2015; Gao & Yang, 2009). After 1999, the implementation of EEPs strongly increased the vegetation regrowth in the region. Although the negative anomalies in SPEI prevail until 2009, the LAI, GPP_{VPM}, and VOD increased significantly despite droughts.

Changes in C stocks can be used as a key indicator of the effectiveness of ecological restoration (Li, Shi, Sa, et al., 2018), with higher C stocks indicating that restoration efforts have been more effective. We also calculated annual aboveground C stocks (in PgC; Figure 4) and C stocks trend (Figure S3) for the study area by summing carbon density estimates from the VOD data set (Liu et al., 2015; Tong et al., 2018). From 1992 to 1999, the annual average aboveground C stock was ~4.94 PgC with a decreasing trend (β = −.11 PgC yr^{-1}, p = .018). After 1999, the annual C stocks increased by ~6.1% to 5.3 PgC in 2012 (β = .05 PgC yr^{-1}, p = .0), despite negative anomalies in SPEI (Figure 3h; Figure S4c1,c2). This result is in line with previous studies (Huang, Liu, Shao, & Deng, 2016), which found that the total C stocks of major terrestrial ecosystems (forests, grasslands, and wetlands) in Northern China had a decreasing trend from 1992 to 2000 and that forest C stocks increased in northwest China after 2000. Our study found that C stocks changed from 5.51 PgC in 1992 to 4.61 PgC in 1999 (−16.3%), with most of the decrease being in forests in the LPS and Greater Khingan Mountain (Figure S3b). Before 1999, substantial deforestation occurred, and grassland was degraded (Huang et al., 2016). After 1999, C stocks increased significantly from 4.6 PgC in 2000 to 5.27 PgC in 2012 (15.1%), especially in LPS and NNS (Figure S3c), with the highest increases in 2002 and 2004 corresponding to the period when multiple large-scale EEPs were implemented in succession. The relationships between these vegetation parameters and temperature and precipitation as potential drivers of the observed changes were analyzed and showed limited explanatory power (see Figure S5).

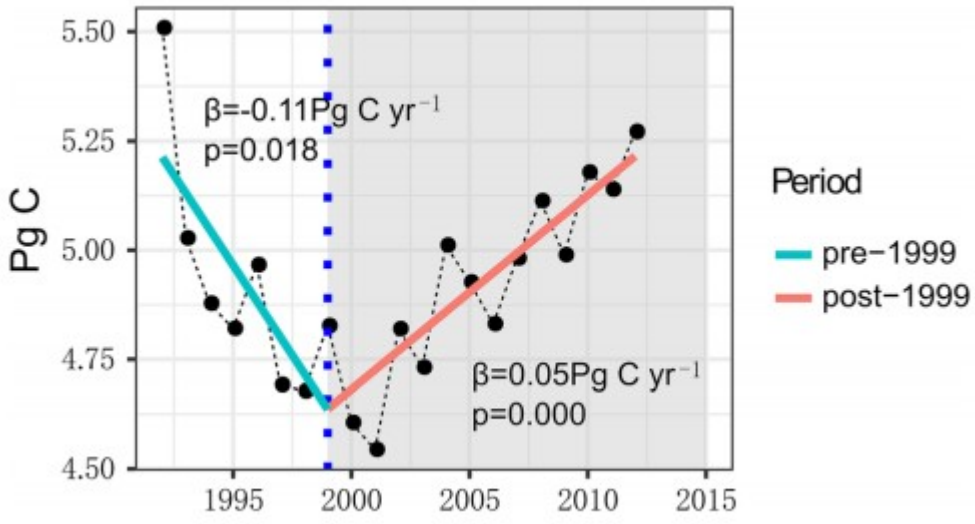

Figure 4. Annual sum carbon stocks estimated from vegetation optical depth. The black point is annual aboveground C stocks (in PgC); the green and orange fit lines are in pre- and post-1999, respectively

3.3 Regional dynamics of LAI, GPP_{VPM}, and VOD trends in 2000s

The dynamics of LAI, GPP_{VPM}, and VOD were generally consistent over the study period, particularly in the 2000s when LAI, GPP_{VPM}, and VOD consistently increased (Figure 3e–g) and the regressions between them indicated that they were positively correlated (Figure S6). Most areas with significant increasing trends were in southern LPS (III), northern NNS (II), and eastern WNS (I). However, LAI had slightly decreasing trends in Inner Mongolia (IM), Greater Khingan Mountains, Hulun Buir, and Horqin Sand Land (Figure 5a). The trend in GPP_{VPM} for these areas was nearly flat (Figure 5b), and decreasing trends in VOD were observed (Figure 5c) in high-altitude, dry areas where overgrazing and droughts may have caused vegetation regrowth to stall. Urban areas were found to show a significant decreasing trend in LAI, especially in Tianjin City. Negative trends in IM and Horqin Sandy Land were mainly in areas of meadow steppe and typical steppe (Figure 5d), which agreed with previous studies (Kang, Han, Zhang, & Sun, 2007; Qin et al., 2015). The degraded areas may be caused by overgrazing and/or drought, indicating that these EEPs have had no obvious impact on vegetation regrowth in these areas.

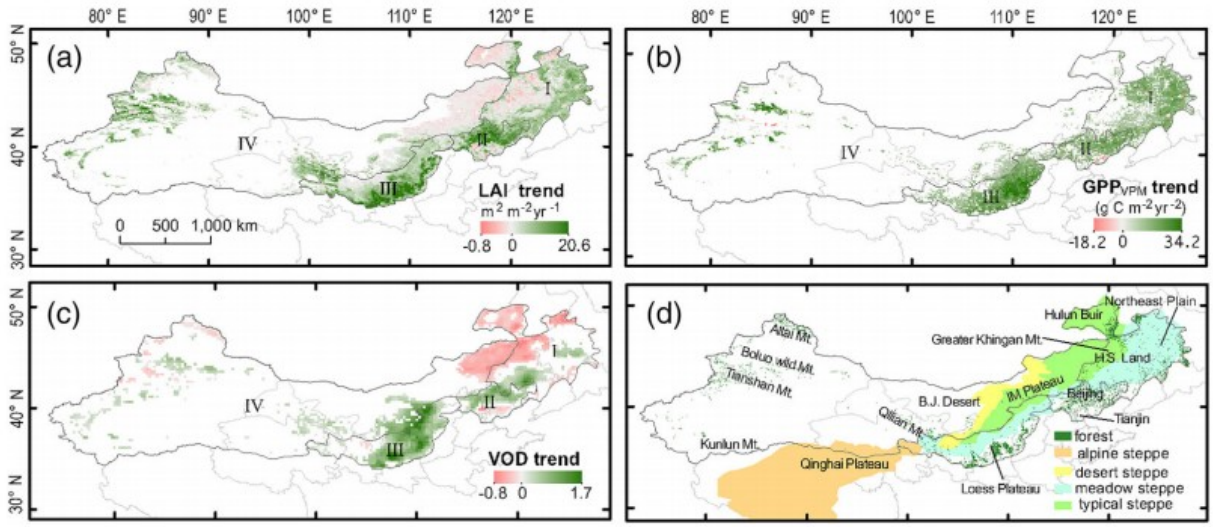

Figure 5. Vegetation trends and vegetation types in the study area. (a) Leaf area index (LAI) trends (p value < .05, n = 35) from 1982 to 2016. (b) GPP_{VPM} trends (p value < .05, n = 17) from 2000 to 2016. (c) Vegetation optical depth (VOD) trends (p value < 0.05, n = 21) from 1992 to 2012. (d) Vegetation types. White areas (Figure a–c) represent the slope is close to zero or bare ground

To further analyze the restoration efforts in the region, we calculated the average trends from LAI, GPP_{VPM}, VOD, and SPEI per subregion during the two periods, pre- and post-1999 (Figure 6; Figure S4). Before 1999, the average trends from VOD in all subregions were lower than post-1999, and the same results were measured from LAI except in MXS. After 1999 (Figure 6a; Table 1), LAI trends in LPS had a larger rate of increase of 0.034 $m^2\ m^{-2}\ yr^{-1}$, and in WNS and NNS the rates of increase were 0.005 $m^2\ m^{-2}\ yr^{-1}$ and 0.01 $m^2\ m^{-2}\ yr^{-1}$, respectively. A slight decreasing trend in LAI was observed in MXS, which coincided with drought (Figure 6d; Figure S4). VOD trends in LPS and NNS had a stronger increase than MXS and WNS (Figure 6c). Field surveys indicated that a lot of natural and planted forests are found in LPS and NNS, whereas croplands and meadows are mainly found in WNS and MXS (Figure 5d), contributing to the VOD trends in LPS and NNS. C-stock trends also showed the same result (Table 1), and the ΔC-stock trends in LPS and NNS were 0.6093 TgC yr^{-1} and 0.7332 TgC yr^{-1}, respectively. Statistics from GPP_{VPM} trends after 1999 revealed that the vegetation cover increased in LPS and NNS with the trends of 7.2^2 and 6.1 gC yr^{-2}, respectively. At the provincial level (Table S2), five provinces (Liaoning, Shannxi, Hebei, Beijing, and Heilongjiang) had positive LAI trends before 1999. However, for the C-stock trends, all provinces except Qinghai and Xinjiang had a weak negative C-stock trend. After 1999, only IM had a slightly negative LAI trend, whereas all provinces had positive GPP_{VPM} trends. Negative C-stock trends occurred in Tianjin and Xinjiang post-1999.

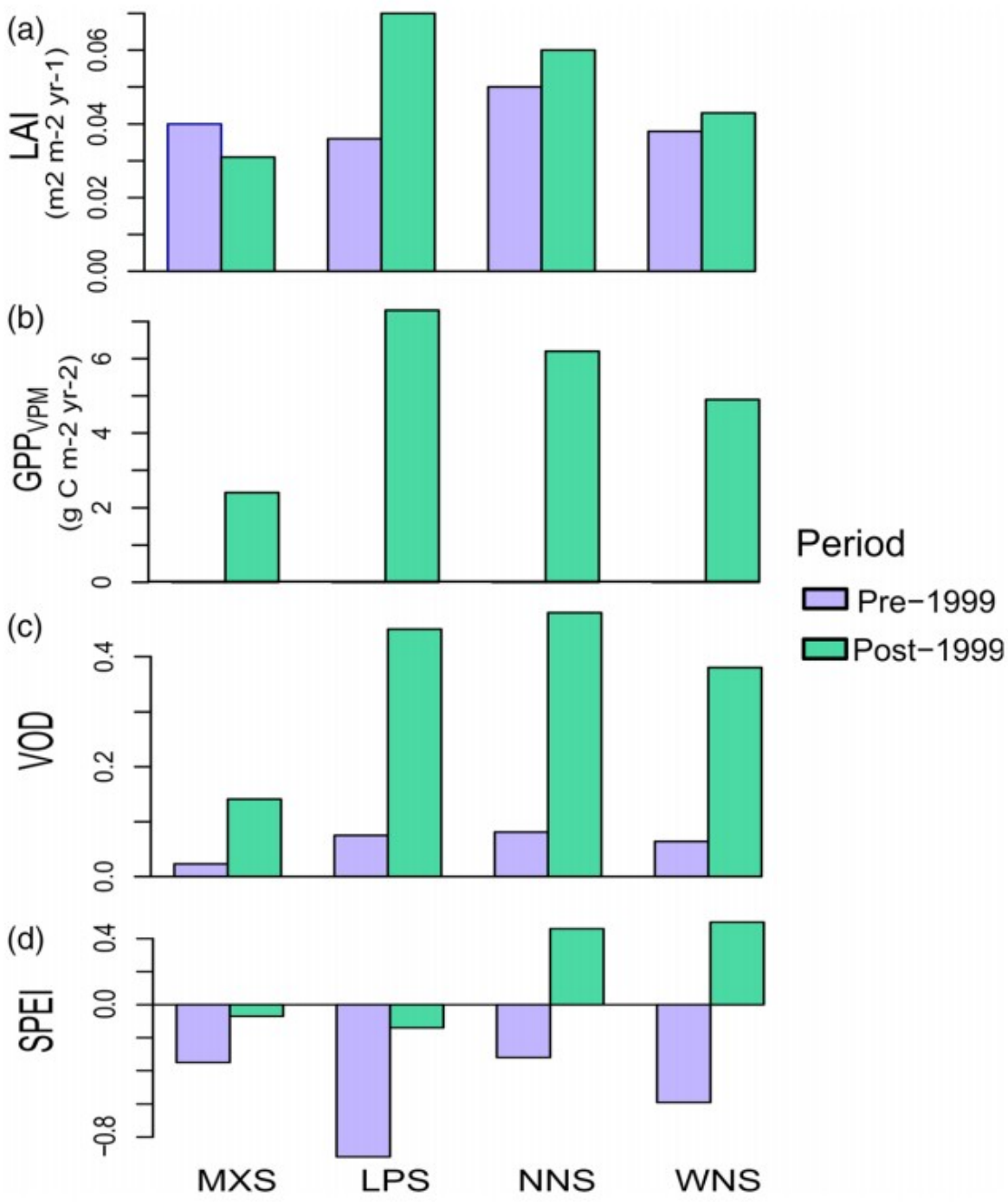

Figure 6. Average trends pre and post 1999 at the subregional level (p value < .05). (a) leaf area index (LAI; 1982–2016), (b) gross primary production data set from the Vegetation Photosynthesis Model (GPP_{VPM}; 2000–2016), (c) vegetation optical depth (VOD; 1992–2012); (d) standardized precipitation-evapotranspiration index (SPEI; 1982–2015)

4 DISCUSSIONS

4.1 EEPs effect on vegetation regrowth

In semiarid and subhumid Northern China, our results showed that multiple EEPs led to considerable increases in vegetation regrowth, which is consistent with findings from other studies (Y. Zhang et al., 2016; Zheng & Zhu, 2013). Increases in LAI, GPP_{VPM}, and VOD were detected in the study region where multiple large-scale EEPs were implemented during the study period. However, areas with vegetation degradation were identified on plateaus, sandy lands, and in urban areas. Prior to the implementation of ecological projects, vegetation cover in the southeast area of the study region was low, and desertification and dust-storms caused severe problems in Northern China (Li et al., 2012; Piao, 2003; Wang et al., 2010). The breakpoints of vegetation shifts in LAI time-series showed substantially larger areas with a monotonic increase than a decrease, and the of breakpoint years showed a geographical succession from south to north during the study period, which coincided with the implementation of multiple large-scale EEPs. The increases in LAI, GPP_{VPM}, and VOD after 1999 occurred despite that Northern China experienced the most severe drought in 60 years during this period (Chen & Sun, 2015; Gao & Yang, 2009). These increases also confirmed the ground-based statistical data available for forest EEPs, which shows a progressive increase in forest area during the study period (Figure S7; Table S1) and that more trees were planted in dry and harsh regions to control dust storms and desertification. To achieve the project aims, the Chinese Government continuously introduced new policies and rules to limit logging and grazing to restore natural and planted forest landscapes. Moreover, increasing investments from the Chinese Government greatly contributed to the greening in the region. For example, the average subsidy for planting trees was 1875.8 CNY/ha in 2000–2007 for the TNSFP, which is 35-times higher than in 1978–1985 (Y. Zhang et al., 2016). The EEP with the largest investment, the GfG, involves an investment of approximately 6,000 CNY ha^{-1}, and in the Yellow River Basin, the average investment for planting trees was about 4,500 CNY ha^{-1} (China Forestry Administration, 2008). After the launch of GfG, other EEPs (e.g., NFCP and BSSCP) have been implemented, and creative systems were also introduced by local administration entities. For example, it was reported that only 15% of the planted trees survived (Cao, 2008); thus, tree-planting rules were continuously revised, and the subsidies were only paid out when the planted trees survived and began to grow. These changes caused workers to take care of the planted trees, thereby increasing the general efficiency of the projects in more recent years.

Vegetation regrowth varied spatially with most positive trends being in western MXS and the southeastern part of the study region. In these regions, the humid conditions and low elevation likely increase the chances of restoration efforts, with effective policies and great investments, which better contributed to the vegetation regrowth. Our result showed that the negative trends were mainly in the IM Plateau, the Hulun Buir Grassland, and the Horqin Sandy Land, where the vegetation cover was mainly composed of

typical steppe and meadow steppe. Little impacts from EEPs were identified in these places, likely due to the dry climate and overgrazing. In MXS, the positive trends were mainly located in the western part, where the largest Farmland Protective Forest Networks have been built. Here, trees have been planted in lines (which divide the farmlands) on 2.54 million ha, which likely contribute to the greening of the entire subregion (Y. Zhang et al., 2016; Zheng & Zhu, 2013). Vegetation regrowth is also pronounced in the southern Qilian Mountains and in the middle of the Yellow River basin, where warm temperatures and water supply from melting snow create favorable growing conditions (Chen, Takeuchi, Xu, Chen, & Xu, 2006). Meanwhile, very weak changes in C stocks were observed in provinces of IM, Ningxia, Gansu, Qinghai, and Xinjiang, which are likely because of droughts offsetting the planting efforts. In general, large areas with positive trends for vegetation regrowth were observed in LPS and NNS, where high investments from the GfG and BSSCP have been made. Another large ecological project, Closing Hillsides to Facilitate Afforestation, was implemented in these places, which aims at converting barren land to forest or grassland. Together with the TNSFP, these EEPs have effectively promoted vegetation restoration, which has been reflected in the increase in C stocks in administrative districts (e.g., Shanxi, Liaoning, Shannxi, Hebei, and Beijing).

4.2 Multiple vegetation parameter assessment of regrowth

Vegetation regrowth in the region caused by EEPs was effectively quantified by long-term satellite-based GIMMS-3g LAI, GPP_{VPM}, and VOD, which are related to vegetation cover, production, and biomass. The scatterplots among satellite derived variables show a consistency of the vegetation dynamics captured. We used the GIMMS-3g LAI data set to identify the breakpoints of vegetation dynamics with a geographical succession from south to north during the study period, which exactly coincided with the succession of EEP implementation schemes. The BFAST seasonal trend analysis of LAI, GPP_{VPM}, and VOD (Figure S8) found that these variables were temporally and spatially consistent and coincided with the period when several large-scale EEPs were implemented. Our results also showed that the dynamics from multiple vegetation parameters were consistent during in the 2000s, and that annual VOD had a decreasing trend in the 1990s but an increasing trend in the 2000s (also shown in C stocks). Before 1999 the rather neutral LAI and the decrease in VOD could be a sign of insufficient project efforts form TNSFP which were additionally offset by the effects of severe droughts, and after 1999 GfG and other EEPs together contributed to vegetation restoration. Therefore, VOD data could be more sensitive to vegetation change and EEPs in the region.

4.3 The future work for EEPs

Although our results from multiple satellite-based time-series data sets showed positive effects of EEPs on vegetation accumulation and production, the effect of changes in climate on vegetation regrowth were only assessed

by a qualitative comparison with SPEI data. Our research showed clear spatiotemporal patterns of vegetation regrowth that generally coincided with the implementation of the EEPs. However, in situ measurements are still necessary to verify the results. Two challenges remain when conducting future studies of the effects of EEPs in the region. One challenge is how to determine to what degree vegetation regrowth is driven by EEPs and climate. Some studies reported that the climate forcing on vegetation change can be singled out by using dynamic vegetation models (Tong et al., 2018; Zhu et al., 2016). However, the ability of such models to assess the direct effect of human activities is poorly constrained. Another challenge is how to identify what tree species caused vegetation change in the region when the breakpoints were identified. Most of Northern China is arid/semiarid, and water shortage severely restricts tree planting, especially in the northwest area of North China. It is therefore pivotal to assess EEPs with up-to-date technology (e.g., higher-resolution satellite imagery and Synthetic Aperture Radar) and in situ surveys to assess the effect of human activities and tree species on vegetation dynamics.

5 CONCLUSIONS

In semiarid and subhumid Northern China, our results from multiple satellite-based time-series data sets showed positive effects of EEPs on vegetation restoration. Significant breakpoints from break point analysis of LAI were observed for over 72.5% of the study area in 1982–2016, which correspond well to when the largest scale EEPs were implemented. The interannual consistency of LAI, GPP_{VPM}, and VOD presented in this study suggested that the implementation of GfG and other EEPs (e.g., NFCP and BSSCP) strongly restored vegetation in the region after 1999 despite droughts. The southern LPS had the largest increase in vegetation growth, followed by the northern parts of NNS. Among these areas, biomass increased more in Shanxi, Liaoning, Shannxi, and Hebei Provinces and Beijing than Xinjiang, IM, Tianjin, and Qinghai Provinces. Our results indicated that multiple large-scale EEPs in the region have increased vegetation cover, production, and AGB, which has led to improved environmental conditions in Northern China.

ACKNOWLEDGMENTS

We are grateful to four anonymous reviewers for providing valuable comments on a previous version of the manuscript. This study was funded by the National Science Foundation of China (Grant No. 41461084, 31860181), the PhD Programs Foundation of Lanzhou University of Technology and China Scholarship Council.

REFERENCES

Brandt, M., Mbow, C., Diouf, A. A., Verger, A., Samimi, C., & Fensholt, R. (2015). Ground- and satellite-based evidence of the biophysical mechanisms behind the greening Sahel. *Global Change Biology*, 21, 1610– 1620. https://doi.org/10.1371/journal.pone.0079205

Brandt, M., Wigneron, J. P., Chave, J., Tagesson, T., Penuelas, J., Ciais, P., … Fensholt, R. (2018). Satellite passive microwaves reveal recent climate-induced carbon losses in African drylands. *Nature Ecology & Evolution*, 2, 827– 835. https://doi.org/10.1038/s41559-018-0530-6

Cao, S. (2008). Why large-scale afforestation efforts in China have failed to solve the desertification problem. *Environmental Science & Technology*, 42(6), 1826– 1831. https://doi.org/10.1021/es0870597

Cao, S., & Wang, G. (2010). Questionable value of planting thirsty trees in dry regions. *Nature*, 465, 31. https://doi.org/10.1038/465031d

Chambers, J. M. (2009). *Software for data analysis: Programming with R* (p. 498). New York: Springer.

Chen, B., Xu, G., Coops, N. C., Ciais, P., Innes, J. L., Wang, G., … Liu, Y. (2014). Changes in vegetation photosynthetic activity trends across the Asia–Pacific region over the last three decades. *Remote Sensing of Environment*, 144, 28– 41. https://doi.org/10.1016/j.rse.2013.12.018

Chen, H., Marter-Kenyon, J., Lopez-Carr, D., & Liang, X. Y. (2015). Land cover and landscape changes in Shaanxi Province during China's Grain for Green Program (2000-2010). *Environmental Monitoring and Assessment*, 187(10), 644. https://doi.org/10.1007/s10661-015-4881-z

Chen, H., & Sun, J. (2015). Changes in Drought Characteristics over China Using the Standardized Precipitation Evapotranspiration Index. *Journal of Climate*, 28(13), 5430– 5447. https://doi.org/10.1175/jcli-d-14-00707.1

Chen, Y. N., Takeuchi, K., Xu, C. C., Chen, Y. P., & Xu, Z. X. (2006). Regional climate change and its effects on river runoff in the Tarim Basin, China. *Hydrological Processes*, 20(10), 2207– 2216. https://doi.org/10.1002/hyp.6200

China Forestry Administration (1987). Bureau of Three Norths Shelterbelt Development Program, (In Chinese).

China Forestry Administration (2008). *Development report for the three-north shelterbelt system in the past 30 years: 1978–2008*. Beijing: China Forestry Press. (In Chinese).

Cleveland, R. B., Cleveland, W. S., McRae, J. E., & Terpenning, I. (1990). STL: A seasonal trend decomposition procedure based on loess. *Journal of Official Statistics*, 6(1), 3– 33.

de Jong, R., de Bruin, S., de Wit, A., Schaepman, M. E., & Dent, D. L. (2011). Analysis of monotonic greening and browning trends from global NDVI time-series. *Remote Sensing of Environment*, 115(2), 692– 702. https://doi.org/10.1016/j.rse.2010.10.011

de Jong, R., Verbesselt, J., Zeileis, A., & Schaepman, M. E. (2013). Shifts in global vegetation activity trends. *Remote Sensing*, 5, 1117– 1133. https://doi.org/10.3390/rs5031117

Delang, C. O., & Wang, W. (2013). Chinese forest policy reforms after 1998: The case of the natural forest protection program and the slope land conversion program. *International Forestry Review*, 15(Raich et al.), 290–304. https://doi.org/10.1505/146554813807700128

Delang, C. O., & Yuan, Z. (2015). China's reforestation and rural development programs. In *China's Grain for Green Program*. Cham: Springer. https://doi.org/10.1007/978-3-319-11505-4_2

Eckert, S., Hüsler, F., Liniger, H., & Hodel, E. (2015). Trend analysis of MODIS NDVI time series for detecting land degradation and regeneration in Mongolia. *Journal of Arid Environments*, 113, 16– 28. https://doi.org/10.1016/j.jaridenv.2014.09.001

Fan, B., Guo, L., Li, N., Chen, J., Lin, H., Zhang, X., … Ma, L. (2014). Earlier vegetation green-up has reduced spring dust storms. *Scientific Reports*, 4, 6749. https://doi.org/10.1038/srep06749

Fensholt, R., Langanke, T., Rasmussen, K., Reenberg, A., Prince, S. D., Tucker, C., … Wessels, K. (2012). Greenness in semi-arid areas across the globe 1981-2007—An Earth observing satellite based analysis of trends and drivers. *Remote Sensing of Environment*, 121, 144– 158. https://doi.org/10.1016/j.rse.2012.01.017

Fernandes, R., Butson, C., Leblanc, S., & Latifovic, R. (2003). Landsat-5 TM and Landsat-7 ETM+ based accuracy assessment of leaf area index products for Canada derived from SPOT-4 VEGETATION data. *Canadian Journal of Remote Sensing*, 29, 241– 258. https://doi.org/10.5589/m02-092

Galford, G. L., Mustard, J. F., Melillo, J., Gendrin, A., Cerri, C. C., & Cerri, C. E. P. (2008). Wavelet analysis of MODIS time series to detect expansion and intensification of row-crop agriculture in Brazil. *Remote Sensing of Environment*, 112(2), 576– 587. https://doi.org/10.1016/j.rse.2007.05.017

Gao, H., & Yang, S. (2009). A severe drought event in northern China in winter 2008–2009 and the possible influences of La Niña and Tibetan Plateau. *Journal of Geophysical Research*, 114. https://doi.org/10.1029/2009jd012430

Hill, M. J., & Donald, G. E. (2003). Estimating spatio-temporal patterns of agricultural productivity in fragmented landscapes using AVHRR NDVI time series. *Remote Sensing of Environment*, 84(3), 367384. https://doi.org/10.1016/s0034-4257(02)00128-1

Huang, L., Liu, J. Y., Shao, Q. Q., & Deng, X. Z. (2016). Temporal and spatial patterns of carbon sequestration services for primary terrestrial ecosystems in China between 1990 and 2030. *Acta Ecologica Sinica*, 36(13), 3891– 3902 (In Chinese). https://doi.org/10.5846/stxb201411012141

Jiang, B., Liang, S., & Yuan, W. (2015). Observational evidence for impacts of vegetation change on local surface climate over northern China using the

Granger causality test. *European Journal of Vascular and Endovascular Surgery* 2014, 120, JG002741. https://doi.org/10.1002/2014JG002741

Jönsson, P., & Eklundh, L. (2002). Seasonality extraction by function fitting to time-series of satellite sensor data. *IEEE Transactions on Geoscience and Remote Sensing*, 40(8), 1824– 1832. https://doi.org/10.1109/TGRS.2002.802519

Kang, L., Han, X., Zhang, Z., & Sun, O. J. (2007). Grassland ecosystems in China: review of current knowledge and research advancement. *Philosophical Transactions of the Royal Society of London. Series B, Biological Sciences*, 362, 997– 1008. https://doi.org/10.1098/rstb.2007.2029

Li, F., Shi, H., Sa, L., Liu, M., Feng, X., & Li, M. (2018). Reseach on spatial distribution characteristics of forest vegetation carbon density. *Journal of Xi'an University of Architecture & Technology (Natural Science Edition)*, 50, 416– 422. (In Chinese).

Li, M., Liu, A., Zou, C., Xu, W., Shimizu, H., & Wang, K. (2012). An overview of the “Three-North” Shelterbelt project in China. *Forestry Studies in China*, 14(1), 70– 79. https://doi.org/10.1007/s11632-012-0108-3

Liu, Y. Y., de Jeu, R. A. M., McCabe, M. F., Evans, J. P., & van Dijk, A. I. J. M. (2011). Global long-term passive microwave satellite-based retrievals of vegetation optical depth. *Geophysical Research Letters*, 38, L18402. https://doi.org/10.1029/2011GL048684

Liu, Y. Y., van Dijk, A. I. J. M., de Jeu, R. A. M., Canadell, J. G., McCabe, M. F., Evans, J. P., & Wang, G. (2015). Recent reversal in loss of global terrestrial biomass. *Nature Climate Change*, 5, 470– 474. https://doi.org/10.1038/nclimate2581

Ma, H., Lv, Y., & Li, H. (2013). Complexity of ecological restoration in China. *Ecological Engineering*, 52, 75– 78. https://doi.org/10.1016/j.ecoleng.2012.12.093

Neigh, C. S. R., Tucker, C. J., & Townshend, J. R. G. (2008). North American vegetation dynamics observed with multi-resolution satellite data. *Remote Sensing of Environment*, 112, 1749– 1772. https://doi.org/10.1016/j.rse.2007.08.018

Piao, S., Nan, H., Huntingford, C., Ciais, P., Friedlingstein, P., Sitch, S., … Chen, A. (2014). Evidence for a weakening relationship between interannual temperature variability and northern vegetation activity. *Nature Communications*, 5, 5018. https://doi.org/10.1038/ncomms6018

Piao, S., Yin, G., Tan, J., Cheng, L., Huang, M., Li, Y., … Wang, Y. (2015). Detection and attribution of vegetation greening trend in China over the last 30 years. *Global Change Biology*, 21, 1601– 1609. https://doi.org/10.1111/gcb.12795

Piao, S. (2003). Interannual variations of monthly and seasonal normalized difference vegetation index (NDVI) in China from 1982 to 1999. *Journal of Geophysical Research*, 108. https://doi.org/10.1029/2002jd002848

Qin, Y., Xiao, X., Dong, J., Zhang, G., Shimada, M., Liu, J., … Moore, B. (2015). Forest cover maps of China in 2010 from multiple approaches and data sources: PALSAR, Landsat, MODIS, FRA, and NFI. *ISPRS Journal of Photogrammetry and Remote Sensing*, 109, 1– 16. https://doi.org/10.1016/j.isprsjprs.2015.08.010

Qiu, B., Chen, G., Tang, Z., Lu, D., Wang, Z., & Chen, C. (2017). Assessing the Three-North Shelter Forest Program in China by a novel framework for characterizing vegetation changes. *ISPRS Journal of Photogrammetry and Remote Sensing*, 133, 75– 88. https://doi.org/10.1016/j.isprsjprs.2017.10.003

Schaphoff, S., Forkel, M., Müller, C., Knauer, J., von Bloh, W., Gerten, D., … Waha, K. (2017). LPJmL4 – a dynamic global vegetation model with managed land: Part II – Model evaluation. *Geoscientific Model Development Discussion*, 1– 41. https://doi.org/10.5194/gmd-2017-146

Sun, G., Zhou, G., Zhang, Z., Wei, X., McNulty, S. G., & Vose, J. M. (2006). Potential water yield reduction due to forestation across China. *Journal of Hydrology*, 328, 548– 558. https://doi.org/10.1016/j.jhydrol.2005.12.013

Tan, M., & Li, X. (2015). Does the Green Great Wall effectively decrease dust storm intensity in China? A study based on NOAA NDVI and weather station data. *Land Use Policy*, 43, 42– 47. https://doi.org/10.1016/j.landusepol.2014.10.017

Tian, F., Brandt, M., Liu, Y. Y., Verger, A., Tagesson, T., Diouf, A. A., … Fensholt, R. (2016). Remote sensing of vegetation dynamics in drylands: Evaluating vegetation optical depth (VOD) using AVHRR NDVI and in situ green biomass data over West African Sahel. *Remote Sensing of Environment*, 177, 265– 276. https://doi.org/10.1016/j.rse.2016.02.056

Tong, X., Brandt, M., Yue, Y., Horion, S., Wang, K., Keersmaecker, W. D., … Fensholt, R. (2018). Increased vegetation growth and carbon stock in China karst via ecological engineering. *Nature Sustainability*, 1, 44– 50. https://doi.org/10.1038/s41893-017-0004-x

Verbesselt, J., Hyndman, R., Newnham, G., & Culvenor, D. (2010). Detecting trend and seasonal changes in satellite image time series. *Remote Sensing of Environment*, 114, 106– 115. https://doi.org/10.1016/j.rse.2009.08.014

Verbesselt, J., Hyndman, R., Zeileis, A., & Culvenor, D. (2010). Phenological change detection while accounting for abrupt and gradual trends in satellite image time series.pdf. *Remote Sensing of Environment*, 114, 2970– 2980. https://doi.org/10.1016/j.rse.2010.08.003

Vicente-Serrano, S. M., Tomas-Burguera, M., Beguería, S., Reig, F., Latorre, B., Peña-Gallardo, M., … González-Hidalgo, J. C. (2017). A high resolution

dataset of drought indices for Spain. *Data*, 2, 22. https://doi.org/10.3390/data2030022

Wang, X. M., Zhang, C. X., Hasi, E., & Dong, Z. B. (2010). Has the Three Norths Forest Shelterbelt Program solved the desertification and dust storm problems in arid and semiarid China? *Journal of Arid Environments*, 74, 13– 22. https://doi.org/10.1016/j.jaridenv.2009.08.001

Weiss, J. L., Gutzler, D. S., Coonrod, J. E. A., & Dahm, C. N. (2004). Long-term vegetation monitoring with NDVI in a diverse semi-arid setting, central New Mexico, USA. *Journal of Arid Environments*, 58(2), 249– 272. https://doi.org/10.1016/j.jaridenv.2003.07.001

Wu, Z., Wu, J., He, B., Liu, J., Wang, Q., Zhang, H., & Liu, Y. (2014). Drought offset ecological restoration program-induced increase in vegetation activity in the Beijing-Tianjin Sand Source Region, China. *Environmental Science & Technology*, 48, 12108– 12117. https://doi.org/10.1021/es502408n

Xiao, X. (2004). Modeling gross primary production of temperate deciduous broadleaf forest using satellite images and climate data. *Remote Sensing of Environment*, 91, 256– 270. https://doi.org/10.1016/j.rse.2004.03.010

Xiao, X., Zhang, Q., Hollinger, D., Aber, J., & Moore, B. III (2005). Modeling gross primary production of an evergreen needleleaf forest using MODIS and climate data. *Ecological Applications*, 15(Raich et al.), 954– 969. https://doi.org/10.2307/4543407

Xu, J. T., Yin, R. S., Li, Z., & Liu, C. (2006). China's ecological rehabilitation: Unprecedented efforts, dramatic impacts, and requisite policies. *Ecological Economics*, 57(4), 595– 607. https://doi.org/10.1016/j.ecolecon.2005.05.008

Xu, W. D., & Zou, C. J. (1998). *Sandy forest ecosystems of China*. Beijing: China Forestry Publishing House. (in Chinese).

Yu, K., Li, D., & Li, N. (2006). The evolution of Greenways in China. *Landscape and Urban Planning*, 76, 223– 239. https://doi.org/10.1016/j.landurbplan.2004.09.034

Zhang, X., Huang, T., Zhang, L., Shen, Y., Zhao, Y., Gao, H., … Ma, J. (2016). Three-North Shelter Forest Program contribution to long-term increasing trends of biogenic isoprene emissions in northern China. *Atmospheric Chemistry and Physics*, 16, 6949– 6960. https://doi.org/10.5194/acp-16-6949-2016

Zhang, Y., Peng, C., Li, W., Tian, L., Zhu, Q., Chen, H., … Xiao, X. (2016). Multiple afforestation programs accelerate the greenness in the ‘Three North’ region of China from 1982 to 2013. *Ecological Indicators*, 61, 404– 412. https://doi.org/10.1016/j.ecolind.2015.09.041

Zhang, Y., Xiao, X., Wu, X., Zhou, S., Zhang, G., Qin, Y., & Dong, J. (2017). A global moderate resolution dataset of gross primary production of vegetation for 2000-2016. *Scientific Data*, 4, 170165. https://doi.org/10.1038/srep39748.

Zheng, X., & Zhu, J. (2013). Estimation of shelter forest area in Three-North Shelter Forest Program region based on multi-sensor remote sensing data. *Chinese Journal of Applied Ecology*, 24(8), 2257– 2264. (In Chinese).

Zhou, Z. C., Gan, Z. T., Shangguan, Z. P., & Dong, Z. B. (2009). China's Grain for Green Program has reduced soil erosion in the upper reaches of the Yangtze River and the middle reaches of the Yellow River. *International Journal of Sustainable Development and World Ecology*, 16, 234– 239. https://doi.org/10.1080/13504500903007931

Zhu, Z. (1998). Concept, Cause and Control of Desertification in China. *Quaternary Science*, 2, 145– 155. (In Chinese).

Zhu, Z., Bi, J., Pan, Y., Ganguly, S., Anav, A., Xu, L., … Myneni, R. B. (2013). Global data sets of vegetation leaf area index (LAI)3g and fraction of photosynthetically active radiation (FPAR)3g derived from global inventory modeling and mapping studies (GIMMS) normalized difference vegetation index (NDVI3g) for the period 1981 to 2011. *Remote Sensing*, 5, 927– 948. https://doi.org/10.3390/rs5020927

Zhu, Z., Liu, S., & Di, X. (1989). *Desertification and its control in China*. Beijing: Science Press. (In Chinese).

Zhu, Z., Piao, S., Myneni, R. B., Huang, M., Zeng, Z., Canadell, J. G., … Zeng, N. (2016). Greening of the Earth and its drivers[J]. *Nature Climate Change*, 6(8), 791– 795. https://doi.org/10.1038/nclimate3004